PNAS
www.pnas.org

Supplementary Information for

Retinal Inputs Signal Astrocytes to Recruit Interneurons into Visual Thalamus

Jianmin Su[*], Naomi E. Charalambakis[*], Ubadah Sabbagh, Rachana D. Somaiya, Aboozar Monavarfeshani, William Guido[#], Michael A. Fox[#].

Michael A. Fox

Email: mafox1@vtc.vt.edu

William Guido

Email: william.guido@louisville.edu

This PDF file includes:

Figures S1 to S6

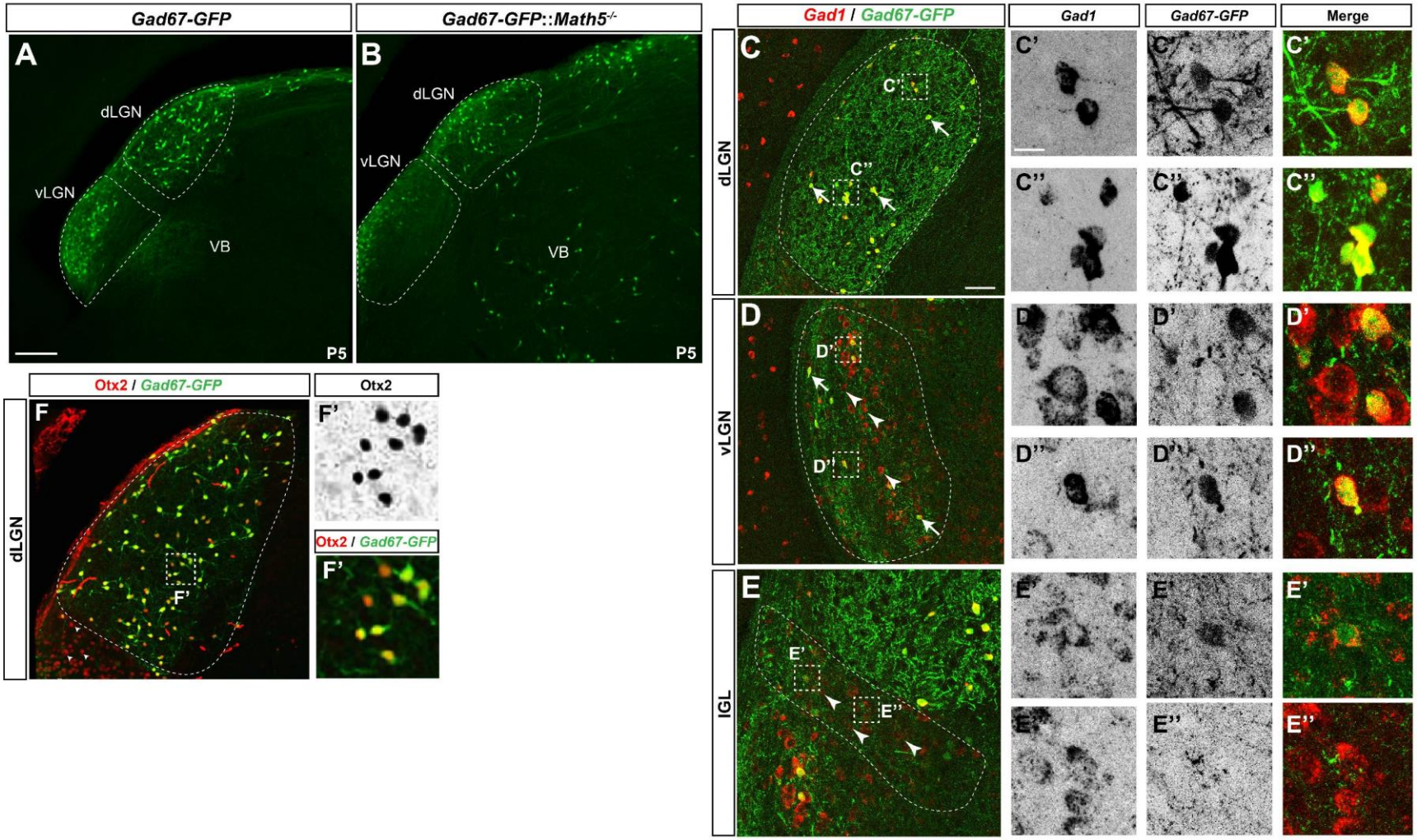
Gad67-GFP
Gad67-GFP::Math5-/-
A
B
dLGN
vLGN
VB
P5
Otx2 / Gad67-GFP
Otx2
F
F'
dLGN
Gad1 / Gad67-GFP
Gad1
Gad67-GFP
Merge
C
C'
C''
D
D'
D''
E
E'
E''
vLGN
IGL

Fig. S1. *Gad67-GFP* labels a subset of GABAergic neurons in visual thalamus.

(A) A subset of GABAergic interneurons in the visual thalamus labeled in *Gad67-GFP* mice. (B) A subset of GABAergic interneurons in the visual thalamus labeled in *Gad67-GFP* ::*Math5*$^{-/-}$. (C-E) Localization of *Gad1* mRNA (*in situ* hybridization) in dLGN (C), vLGN (D), and IGL (E) of interneurons in P22 *Gad67-GFP* mice. White arrowheads indicate *Gad1*$^{+}$GFP^{-} neurons; white arrows indicate *Gad1*$^{+}$GFP^{+} neurons. dLGN, vLGN, and IGL are outlined with dashed lines in C, D, and E, respectively. (F) Immunostaining for Otx2 revealing co-expression in GFP^{+} GABAergic interneurons in dLGN (outlined in white) of *Gad67-GFP* mice. White arrowheads indicate Otx2^{+}GFP^{-} neurons inside IGL. Scale bars: 150 µm A,B; 70 µm for C-F; 20 µm for C',D',E',F'.

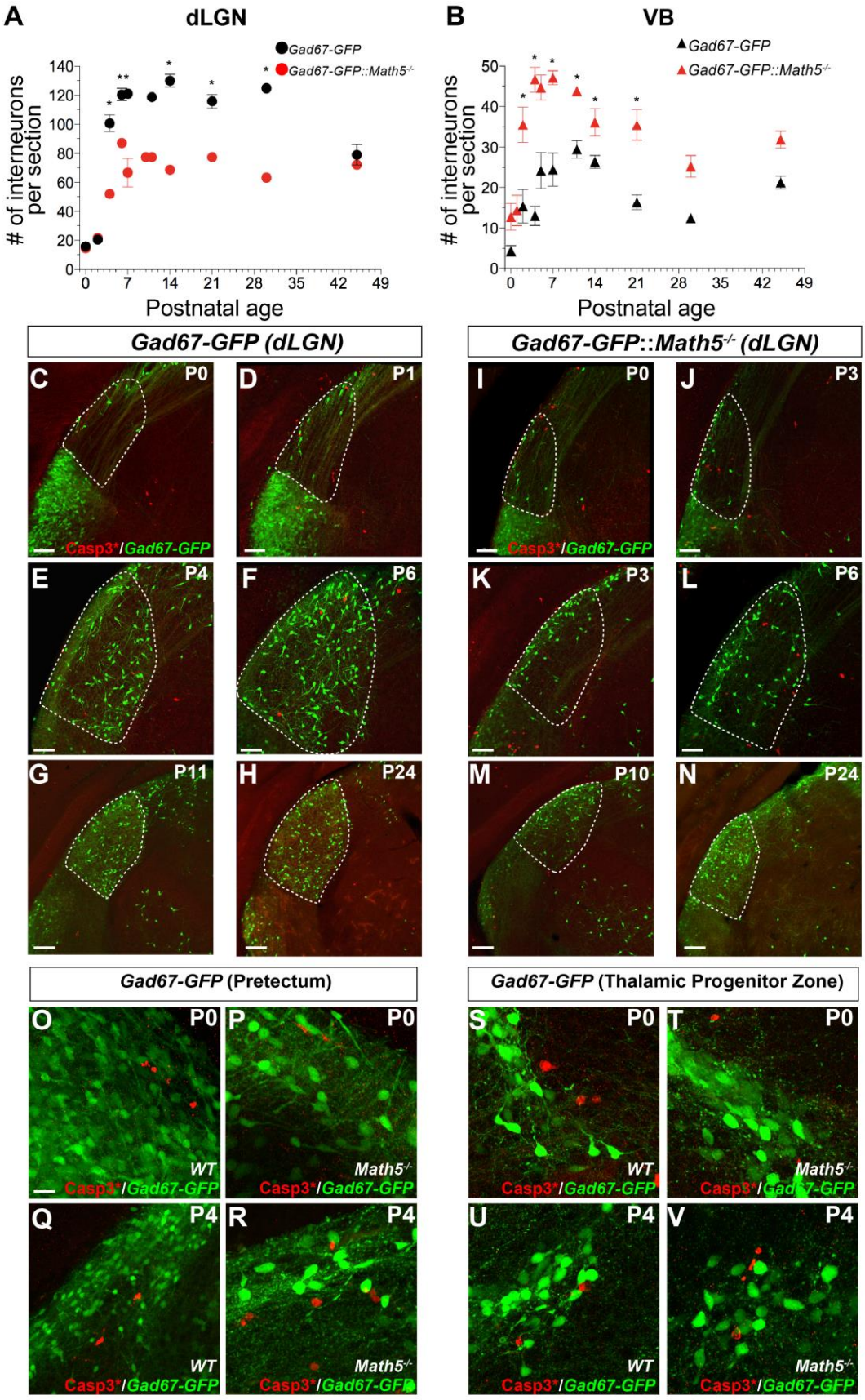
A
dLGN
Gad67-GFP
Gad67-GFP::Math5-/-
# of interneurons per section
Postnatal age
B
VB
Gad67-GFP
Gad67-GFP::Math5-/-
# of interneurons per section
Postnatal age
Gad67-GFP (dLGN)
Gad67-GFP::Math5-/- (dLGN)
C P0
D P1
E P4
F P6
G P11
H P24
I P0
J P3
K P3
L P6
M P10
N P24
Casp3+/Gad67-GFP
Gad67-GFP (Pretectum)
Gad67-GFP (Thalamic Progenitor Zone)
O P0
P P0
Q P4
R P4
S P0
T P0
U P4
V P4
WT
Math5-/-
Casp3+/Gad67-GFP

Fig. S2. Loss of GFP$^+$ interneurons in *Gad67-GFP::Math5$^{-/-}$* mice is due to misrouting, not programmed cell death.

(A-B) Number of GFP$^+$ interneurons throughout the developing dLGN (A) and VB (B) of *Gad67-GFP* and *Gad67-GFP::Math5$^{-/-}$* mice. Data points indicate mean ± SEM. Asterisks (*) represent significance ($p<0.001$) between control and mutant (Two-Way ANOVA). (C-N) Immunostaining for cleaved Caspase 3 (Casp3*) in dLGN of P0-P24 *Gad67-GFP* mice. Note the sparse Casp3* immunoreactivity in visual thalamus of both *Gad67-GFP* and *Gad67-GFP::Math5$^{-/-}$* mice. (O-R) Immunostaining for cleaved Caspase 3 (Casp3*) in the pretectal migratory path of neonatal *Gad67-GFP* and *Gad67-GFP::Math5$^{-/-}$* mice indicating no apoptosis of GFP$^+$ cells along that route. (S-V) Immunostaining for cleaved Caspase 3 (Casp3*) in the thalamic migratory path of neonatal *Gad67-GFP* and *Gad67-GFP::Math5$^{-/-}$* mice indicating no apoptosis of GFP$^+$ cells along that route. Scale bars = 70 µm for C-F, I-L; 150 µm for G, H, M, N; 20 µm for O-V.

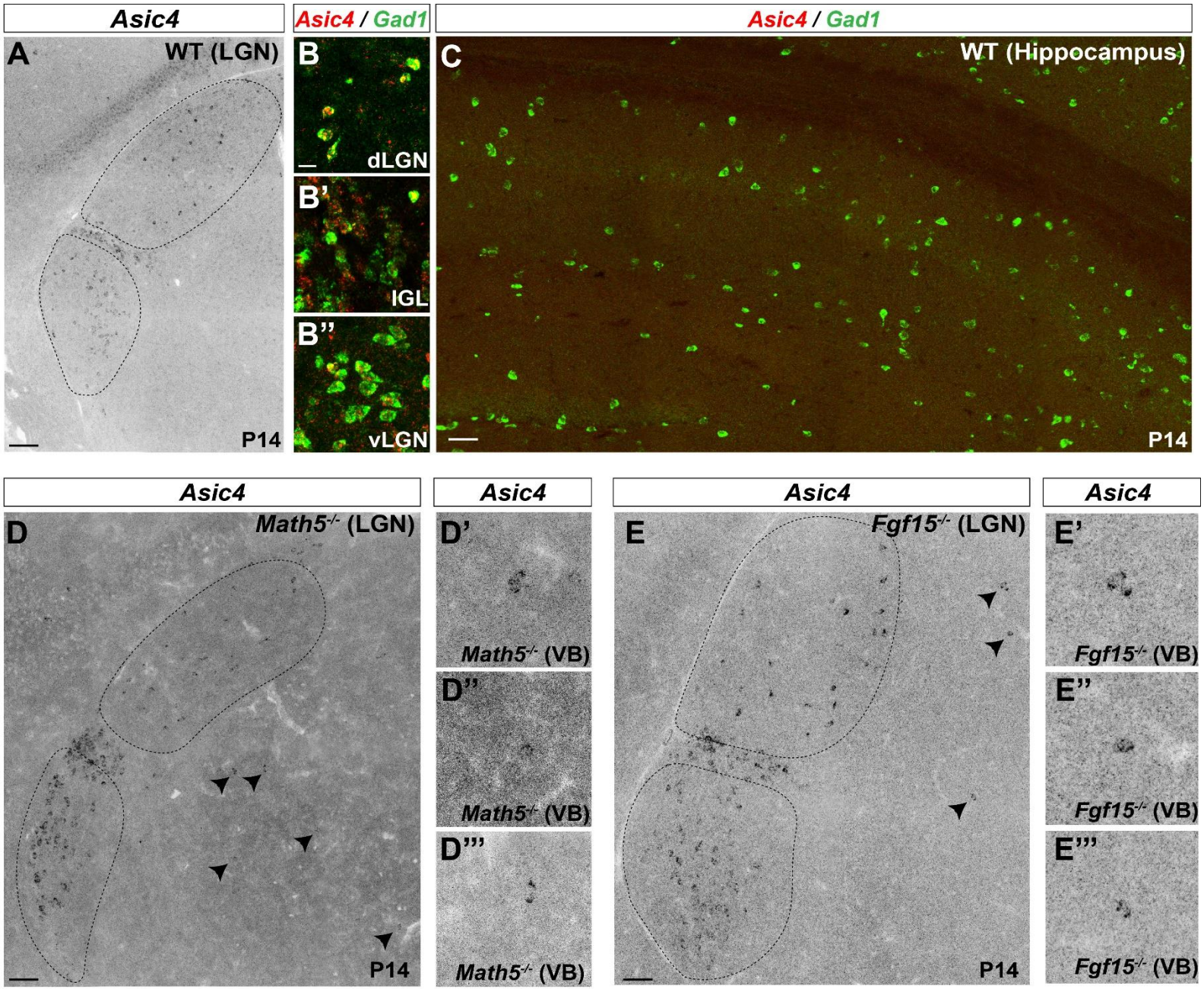
Asic4
A
WT (LGN)
P14
Asic4 / Gad1
B
dLGN
B'
IGL
B''
vLGN
Asic4 / Gad1
C
WT (Hippocampus)
P14
Asic4
D
Math5-/- (LGN)
P14
Asic4
D'
Math5-/- (VB)
D''
Math5-/- (VB)
D'''
Math5-/- (VB)
Asic4
E
Fgf15-/- (LGN)
P14
Asic4
E'
Fgf15-/- (VB)
E''
Fgf15-/- (VB)
E'''
Fgf15-/- (VB)

Fig. S3. GABAergic interneurons in visual thalamus express *Asic4*.

(A) *In situ* hybridization of *Asic4* mRNA in WT LGN. (B) Double *in situ* hybridization of *Asic4* mRNA and *Gad1* mRNA demonstrating that thalamic GABAergic interneurons express *Asic4.* (C) Double *in situ* hybridization of *Asic4* mRNA and *Gad1* mRNA demonstrating that hippocampal GABAergic neurons do not express *Asic4.* (D) *In situ* hybridization of *Asic4* mRNA in thalamus of *Math5*$^{-/-}$ mutants indicates the presence of *Asic4*$^{+}$ cells in inappropriate thalamic regions (D'-D'''). (E) *In situ* hybridization of *Asic4* mRNA in thalamus of *Fgf15*$^{-/-}$ mutants indicates the presence of *Asic4*$^{+}$ cells in inappropriate thalamic regions (E'-E'''). Scale bars = 70 μm for A,C,D,E; 20 μm for B,D',E'.

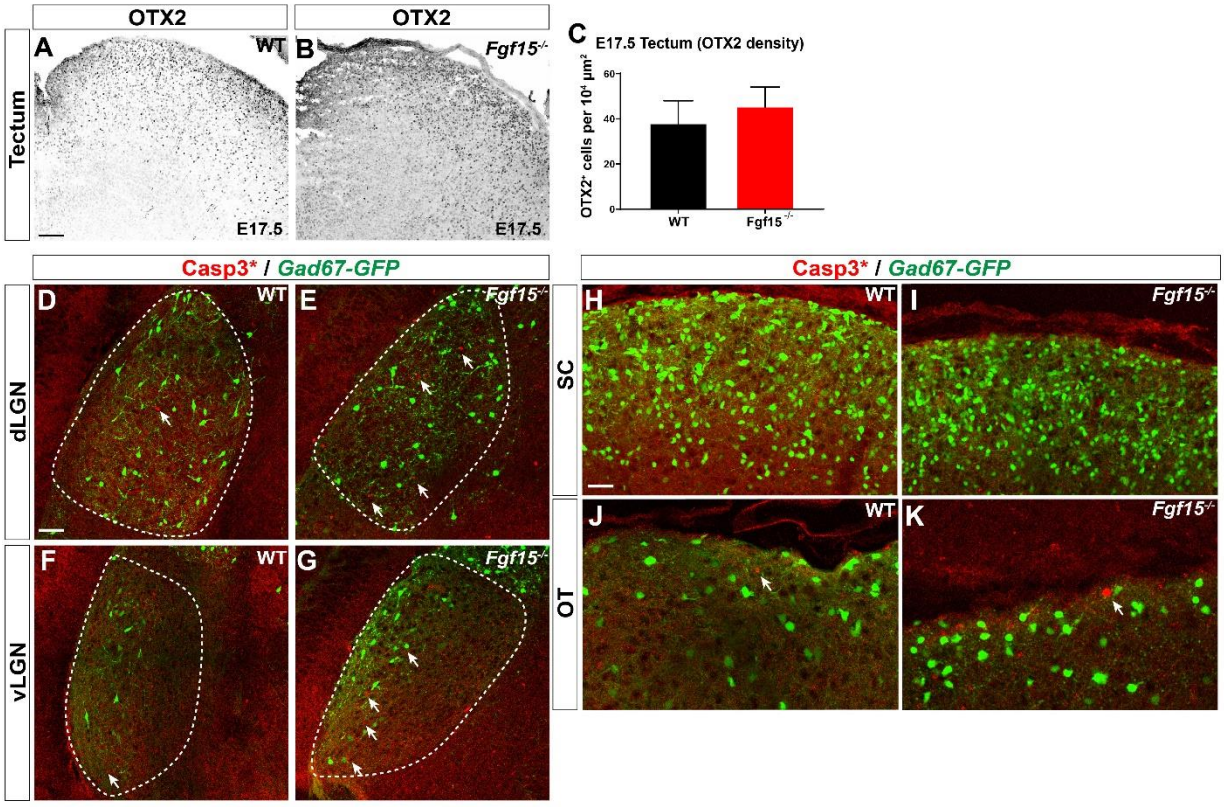
OTX2
OTX2
Tectum
A
WT
B
Fgf15-/-
E17.5
E17.5
C
E17.5 Tectum (OTX2 density)
OTX2+ cells per 10⁴ µm²
60
40
20
0
WT
Fgf15-/-
Casp3* / Gad67-GFP
Casp3* / Gad67-GFP
dLGN
vLGN
SC
OT
D
E
F
G
H
I
J
K
WT
Fgf15-/-

Fig S4. Loss of FGF15 does not impair the generation of OTX2^{+} cells or increase programmed cell death.

(A,B) Immunostaining for OTX2 in embryonic tectum of WT and *Fgf15*$^{-/-}$ mice. (C) Quantification of expression of OTX2^{+} cells in the embryonic tectum of WT and *Fgf15*$^{-/-}$ mice. Data are shown as means ± SEM. (D-G) Immunostaining for cleaved Caspase 3 in LGN of *Gad67-GFP and Gad67-GFP:: Fgf15*$^{-/-}$ mice. (H-I) Immunostaining for cleaved Caspase 3 in tectum of *Gad67-GFP and Gad67-GFP:: Fgf15*$^{-/-}$ mice. (H-I) Immunostaining for cleaved Caspase 3 in tectum of *Gad67-GFP and Gad67-GFP:: Fgf15*$^{-/-}$ mice. (J-K) Immunostaining for cleaved Caspase 3 in optic tract of *Gad67-GFP and Gad67-GFP:: Fgf15*$^{-/-}$ mice. Scale bars = 150 µm for A,B; 70 µm for D-K.

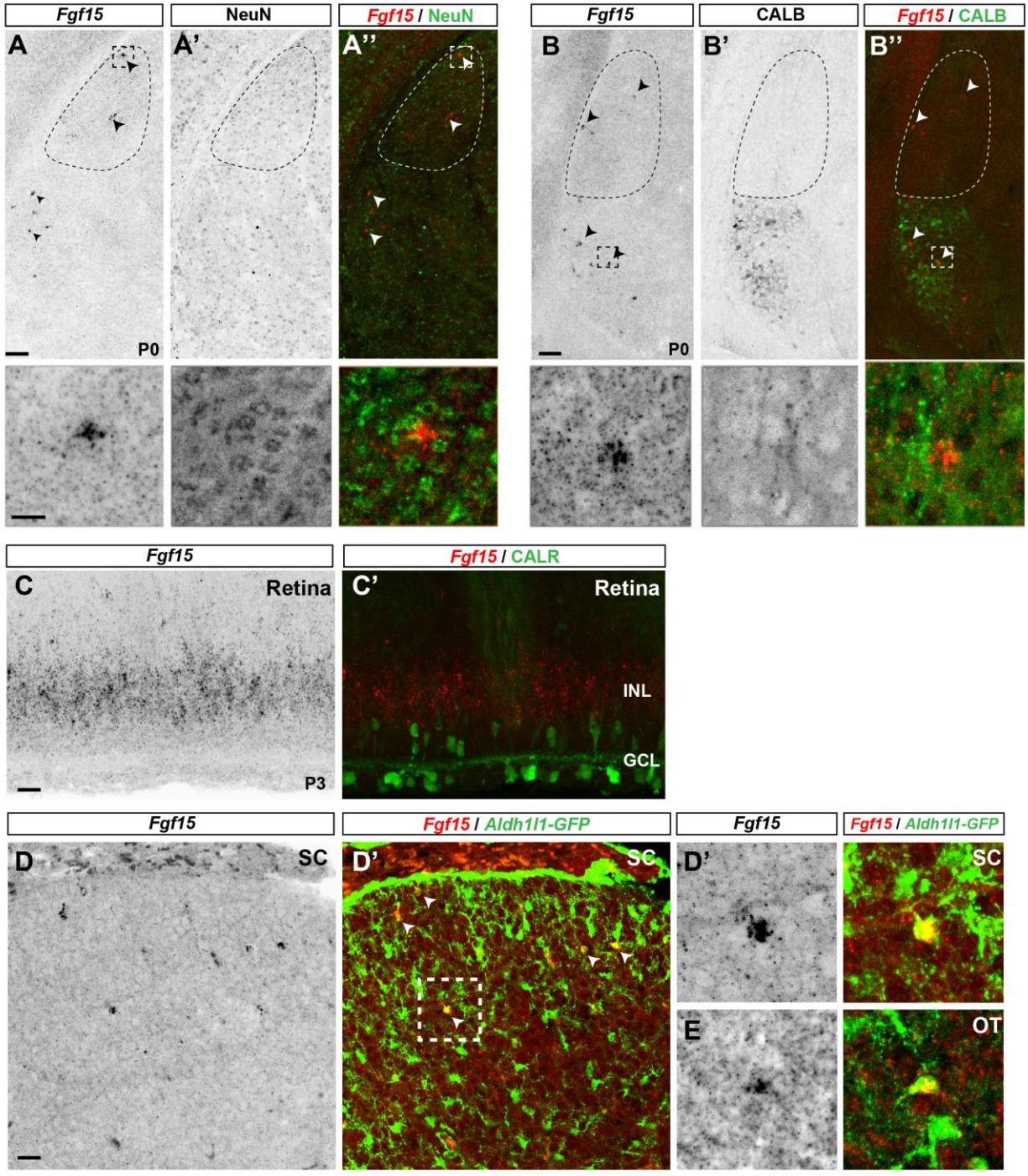
Fgf15
NeuN
Fgf15 / NeuN
A
A'
A''
P0
Fgf15
CALB
Fgf15 / CALB
B
B'
B''
P0
Fgf15
Fgf15 / CALR
C
Retina
P3
C'
Retina
INL
GCL
Fgf15
Fgf15 / Aldh1l1-GFP
Fgf15
Fgf15 / Aldh1l1-GFP
D
SC
D'
SC
D'
SC
E
OT

Fig S5. *Fgf15* is generated by astrocytes and not thalamic neurons or RGCs during neonatal development.

(A) *In situ* hybridization for *Fgf15* and immunostaining for NeuN in P0 visual thalamus (dLGN outlined with dashed lines). White arrowheads indicate *Fgf15*$^{+}$NeuN^{-} cells. (B) *In situ* hybridization for *Fgf15* and immunostaining for CALB in P0 visual thalamus (dLGN outlined with dashed lines). White arrowheads indicate *Fgf15*$^{+}$NeuN^{-} cells. White arrowheads indicate *Fgf15*$^{+}$CALB^{-} cells. (C) *In situ* hybridization for *Fgf15* and immunostaining for CALR in P3 retina. (D) *In situ* hybridization for *Fgf15* in superior colliculus of *Aldh1l1-GFP* mice demonstrating astrocytic expression of *Fgf15*. (E) *In situ* hybridization for *Fgf15* in optic tract of *Aldh1l1-GFP* mice demonstrating astrocytic expression of *Fgf15.* Scale bars: 60 µm for A,B; insets 20 µm. 30 µm for C,D.

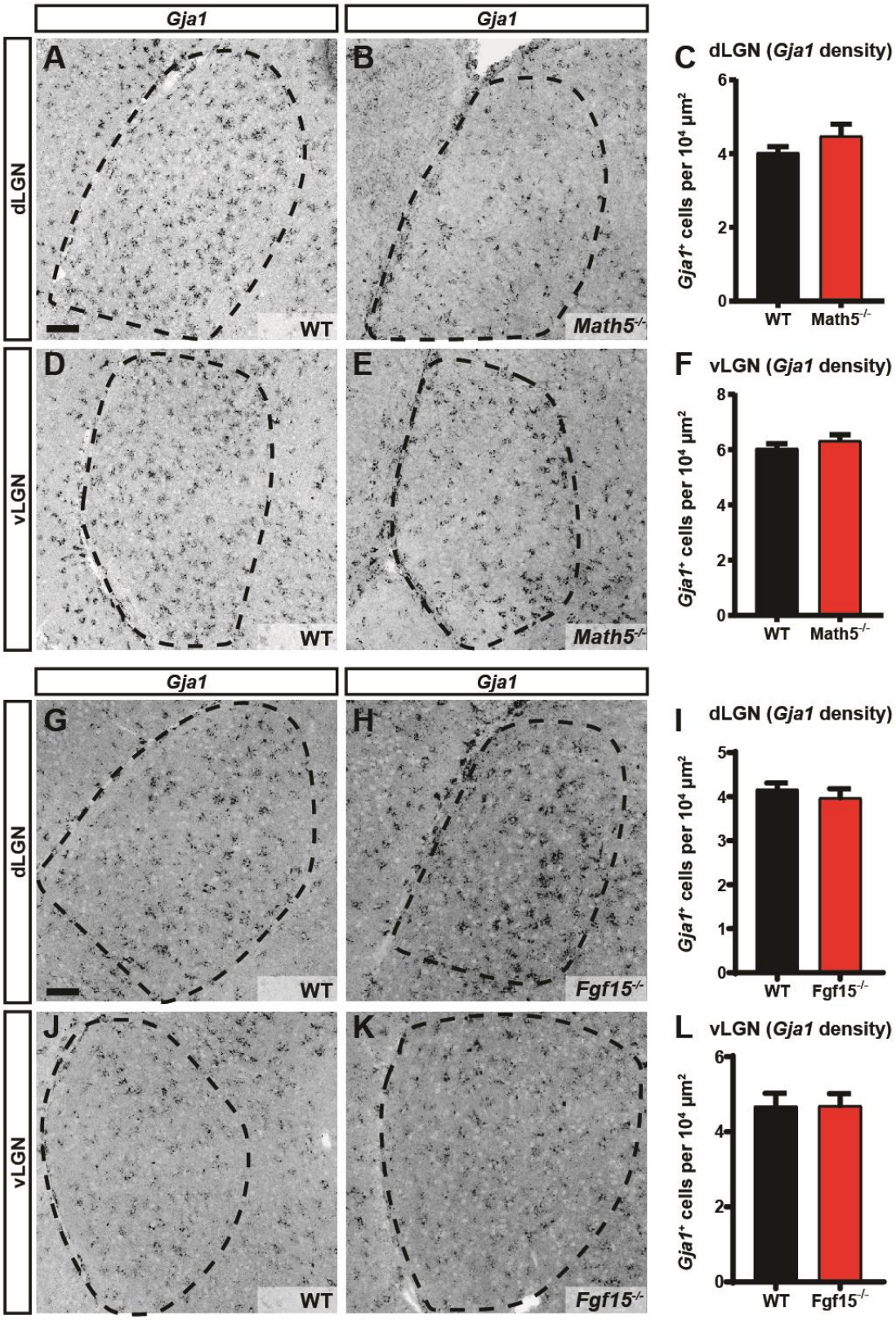
Gja1
Gja1
dLGN
vLGN
A
B
C
D
E
F
G
H
I
J
K
L
WT
Math5-/-
Fgf15-/-
dLGN (Gja1 density)
vLGN (Gja1 density)
Gja1+ cells per 10⁴ µm²
0
2
4
6
8
1
3
5
WT
Math5-/-
Fgf15-/-

Fig S6. Loss of retinal input or *Fgf15* does not impact the distribution of *Gja1*$^{+}$ astrocytes in visual thalamus.

(A,B) In situ hybridization for *Gja1*, a marker of astrocytes, in WT (A) and *Math5-/-* (B) dLGN (outlined with dashed lines). (C) Quantification of *Gja1*-expressing cells in dLGN of WT and *Math5-/-* mice. Data are shown as means ± SEM. (D,E) In situ hybridization for *Gja1*, a marker of astrocytes, in WT (D) and *Math5-/-* (E) vLGN (outlined with dashed lines). (F) Quantification of Gja1-expressing cells in vLGN of WT and *Math5-/-* mice. Data are shown as means ± SEM. (G,H) In situ hybridization for *Gja1*, a marker of astrocytes, in WT (G) and *Fgf15-/-* (H) dLGN (outlined with dashed lines). (I) Quantification of *Gja1*-expressing cells in dLGN of WT and *Fgf15-/-* mice. Data are shown as means ± SEM. (J,K) In situ hybridization for *Gja1*, a marker of astrocytes, in WT (J) and *Fgf15-/-* (K) vLGN (outlined with dashed lines). (L) Quantification of *Gja1*-expressing cells in vLGN of WT and *Fgf15-/-* mice.

Scale bar = 50 µm for A-E; 70 µm for G-K.